

Impact of Micro Orange Glass powder on the Mechanical Properties of SBR and NBR

D. I. Moubarak ¹, Mahmoud Hanafy ², T.Y. El Rasasi ², Y.H. Elbashar ^{3*}

¹ Department of Mechatronics, Faculty of Technological Industry and Energy, Delta Technological University, Qewaisna 32632, Egypt

² Physics Department, Faculty of Science, Benha University, Benha 13518, Egypt

³ Department of Basic Science, ELGazeera High institute for Engineering and Technology, Cairo, Egypt

(*) Corresponding author: y_elbashar@yahoo.com

Abstract

SBR and NBR are widely used in industrial as well as in automobile applications. The main aim of this research is to determine the mechanical properties and their behavior of SBR (Styrene Butadiene Rubber) and NBR (Nitrile Butadiene Rubber) blends mixed with Orange Glass powder as filler) in different compositions. SBR and NBR sheets, and Orange Glass powder are bought and the rubbers are mixed to form blends in order to enhance the properties. Mechanical properties such as tensile, tear, abrasion and resilience tests were conducted according to ASTM standards. Graphs were drawn to compare the results obtained. Enhancement in properties were obtained and noted.

Keywords: SBR NBR polymer, Orange glass, Mechanical properties, glass filler, high elasticity polymer, composites polymer

1. Introduction

The synthetic of natural rubber which made from elastomers. Man-made synthetic rubbers are created from petroleum byproducts and other minerals. Elasticity is the synthetic rubber's primary quality. When under stress, it deforms, but it returns to its original size without suffering any long-term deformation. There are several different varieties of synthetic rubber, including polybutadiene, polybutadiene, polyisoprene, poly chloroprene, Hypalon, SPANDEX, and polysulfide rubber. Pure artificial rubber is useless. Chemical additions can alter the substance's characteristics. The synthetic rubber can be compared to sponge in terms of smoothness, resilience, and hardness. The need for vehicle tires has increased globally, which has led to a rise in the use of synthetic rubber. SBR and nitrile butadiene rubber (NBR) are two of the synthetic rubbers that are most frequently utilized in the automotive sector. The mechanical properties of nitrile butadiene rubber (NBR) and styrene butadiene rubber (SBR) are good but have some restrictions. To improve the qualities of synthetic rubber, many rubber producers today incorporate filler ingredients. By incorporating different varieties of filler material, the mechanical robustness can be altered. Characteristics such as hardness, tensile strength, tear strength, ARI, and rebound resilience can be enhanced through the introduction of said filler.[1-5]. The enhancement of rubber products has been observed when incorporating elastomers in the blending process. The amalgamation of rubbers has the potential to yield novel polymer materials with superior properties. Rubber, being an organic substance, consists of repeating carbon atom units. For this particular study, Nitrile butadiene rubber (NBR) and Styrene butadiene rubber (SBR) have been employed. Nitrile butadiene

rubber (NBR) is classified as a thermoset elastomer. In comparison to other rubber materials, Nitrile butadiene rubber (NBR) exhibits notable thermal conductivity and tensile strength. Similarly, Styrene butadiene rubber (SBR) falls under the category of thermoset elastomers. When compared to alternative materials, Styrene butadiene rubber (SBR) displays a lower density and a greater ductile nature. Moreover, Styrene butadiene rubber (SBR) is suitable for use in abrasive conditions due to its inherent characteristics. It is worth noting that the abrasion nature of Styrene butadiene rubber (SBR) renders it highly resistant to wear and abrasion[6-8]. The synthetic rubber composites exhibit a remarkable aptitude, presenting distinct characteristics suitable for a range of engineering applications, and a substantial ratio of strength to weight. These polymers are employed in diverse engineering applications due to their exceptional properties[9-12]. The introduction of filler material allows for targeted enhancement of the mechanical attributes of these polymers. As such, polymer matrix composites incorporating various types of rubbers and fillers were formulated. The researchers observed improvement in numerous mechanical properties exhibiting a combination of trends. A significant enhancement of up to 20% in both tensile strength and tear strength was achieved by incorporating a mere 5% of fillers. The vulcanization process of Nitrile butadiene rubber (NBR) and Styrene butadiene rubber (SBR) involves the formation of crosslinks, with sulphur serving as the vulcanizing agent. It is important to note that the density of these crosslinks will vary depending on the type of filler used[13-21].

Rubber materials, such as SBR and NBR, are widely utilized in industries due to their excellent properties. To further improve their mechanical properties, the addition of reinforcement fillers is often required. Micro orange glass grains have gained attention as potential fillers that can enhance the mechanical performance of rubber materials. The aim of this work is to investigate the impact of micro orange glass filler grains on the mechanical properties of styrene-butadiene rubber (SBR) and nitrile rubber (NBR). Micro orange glass grains, as a unique type of reinforcement filler, have the potential to enhance the mechanical performance of rubber materials. Understanding their effects on SBR and NBR can provide insights for various industrial applications.

2. Experimental

2.1 materials

Styrene-co- Butadiene rubber (SBR-1502; styrene content, 23.5%) from Transport and Engineering Co. (TRENCO), Alexandria., Egypt., with specific gravity of $1.5 \times 10^3 \text{ kg/m}^3$, glass transition temperature $T_g = -50 \text{ }^\circ\text{C}$, Temperature of vulcanization of $170 \text{ }^\circ\text{C}$, Dielectric constant of 2-3 and Electrical resistivity of $10^{13} \Omega\cdot\text{m}$. Other chemicals were of technical grade such as, Stearic acid as activators with specific gravity at 15°C of $0.9\text{--}0.97 \times 10^3 \text{ kg/m}^3$ was supplied by Aldrich Company, Germany, Zinc oxide (ZnO) as activators with specific gravity at 15°C of $5.55\text{--}5.61 \times 10^3 \text{ kg/m}^3$ was supplied by Aldrich Company, Germany, 2'-Dibenzothiazole Disulfide (MBTS) $\text{C}_{14}\text{H}_8\text{N}_2\text{S}_4$ as accelerator with specific gravity $1.29\text{--}1.31 \times 10^3 \text{ kg/m}^3$, melting point 166°C , and order less powder was supplied by Aldrich Company, Germany, Antioxidant/Antiozonant N-isopropyl N'-cyclohexyl paraphenylene diamine IPPD (4020) purple grey flakes have density $1.17 \times 10^3 \text{ kg/m}^3$ was supplied by Aldrich company, Germany, Naphthenic oil, with specific gravity $0.94\text{--}0.96 \times 10^3 \text{ kg/m}^3$ at 15°C , viscosity $80\text{--}90$ poise at 100°C , and deep green viscous oil was supplied by Aldrich Company, Germany, Elemental sulfur is vulcanizing agent (S) with fine pale yellow powder and specific gravity $2.04\text{--}2.06 \times 10^3 \text{ kg/m}^3$ was supplied by Aldrich company, Germany. Glass powder used as the reinforcing filler is created from non-returnable orange glass bottles. The composites formulation showed in Table 1 and Table 2.

2.2 Measurements

According to ASTM D 3182, all rubber compounds were blended using a milling machine with two 150 mm (diameter) x 300 mm (long) rolls, each with a gear ratio of 1.4 and a slow roll speed of 18 rpm. The vulcanization process was performed after the compounded rubber had been left for 24 hours. Compound rubber is vulcanised in an electrically heated platen hydraulic press at $(143 \pm 2)^\circ\text{C}$ for 20 minutes. Mechanical characteristics including Young's modulus tensile strength, elongation at break, and the different mixes of stress-strain curves were recorded using a homemade tensile testing equipment with a cross head speed of 115 mm/min as shown in (Figure 1). The machine quality improved and measurement errors decreased as a result of the creation of an electronic strain gauge based on the ATMEL 89S52 microprocessor. A rotating wheel and a micromechanical switch with four pulses per revolution (0.789 mm for each switch pulse) were used to measure the displacement of strain. In four-segment auto-range displays, the incoming data is shown. Determination of the abrasion resistance for rubbers and elastomers are performed according to standard DIN 53516 using homemade abrasion tester (fig.2). Shore durometer hardness determination A regime was used with the NT-6510 Shore Hardness Tester (Fig. 3) for five specimens of each sample, each of which was a 3 cm diameter and 1.2 cm thick disc. The experiments were carried out at ambient temperature $(25 \pm 1)^\circ\text{C}$. An average of three samples was collected for each measurement point.

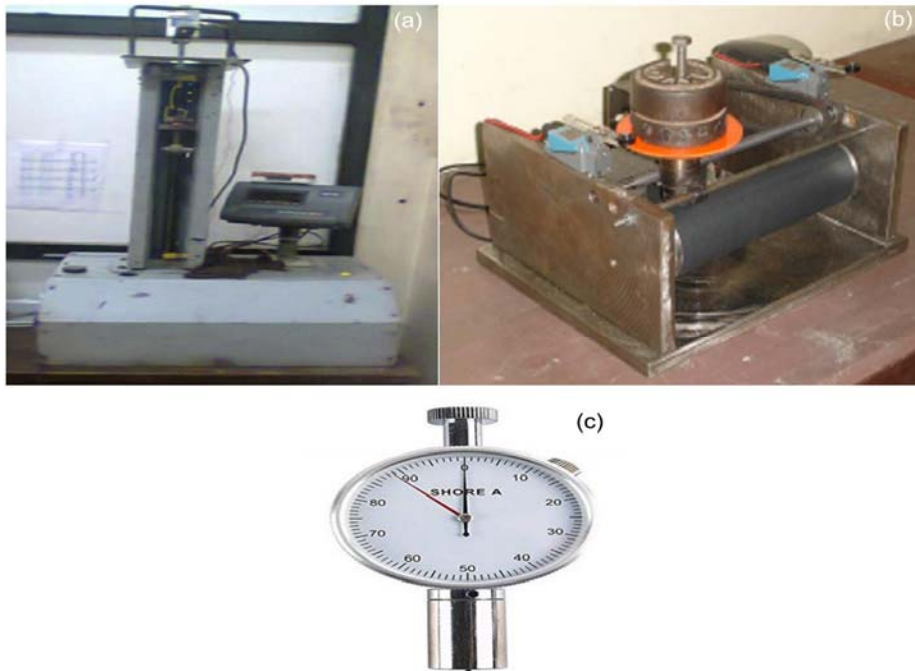


Figure 1 tensile testing equipment, b-abrasion tester and c- shore A

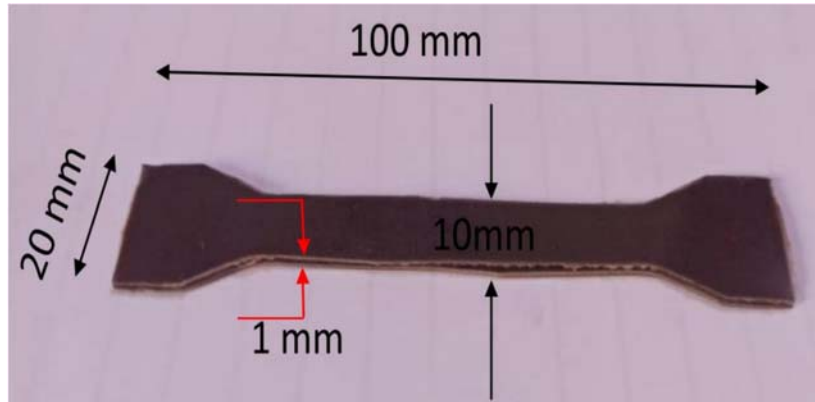


Figure 2 dumbbell shape sample used to obtain tensile – strain characteristics

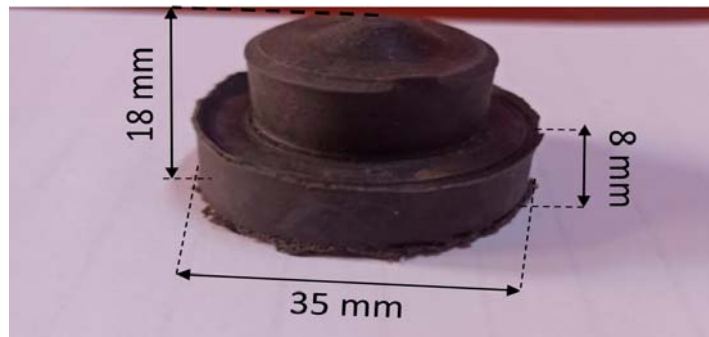


Figure 3 shape of samples with dimensions used for abrasion test

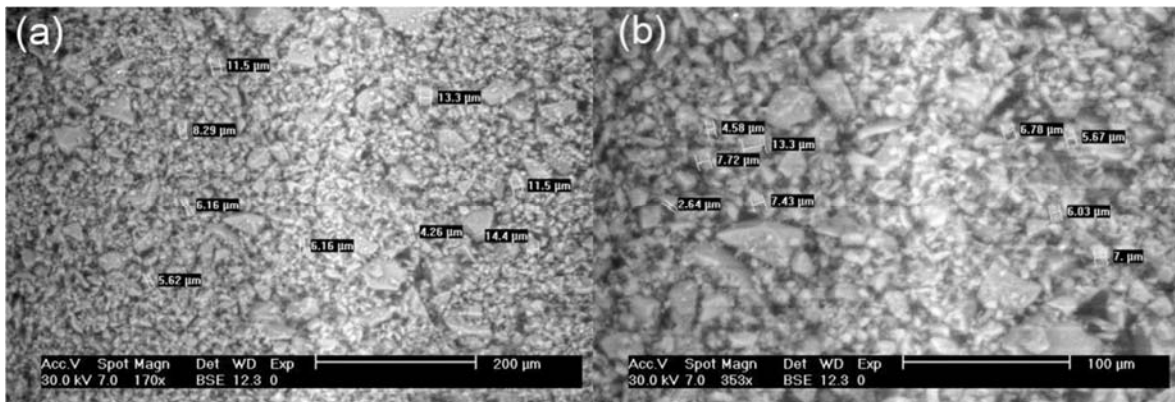


Fig. 4 (a) SEM micrographs of the milled glass in range of 200 μm (b) SEM micrographs of the milled glass in range of 100 μm

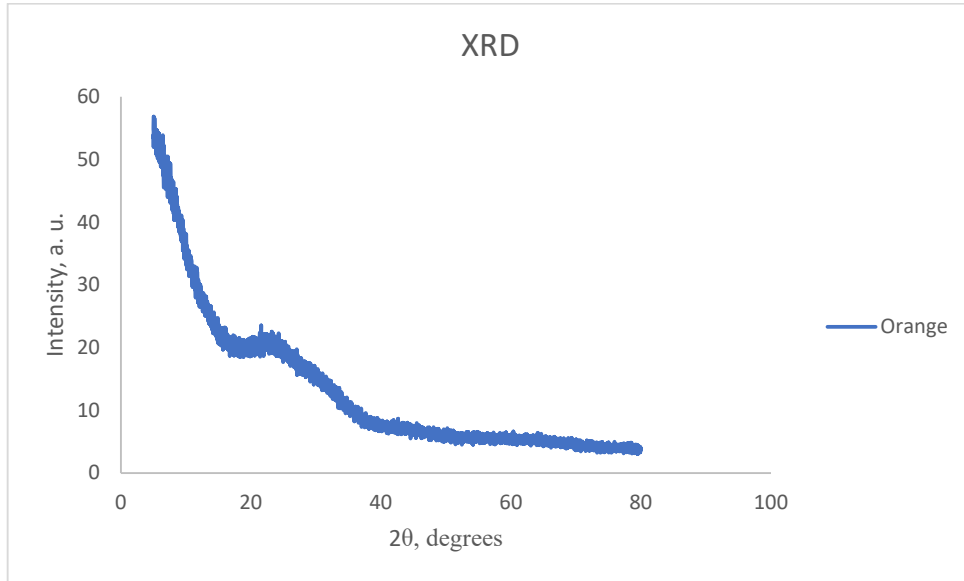


Fig. 5 XRD for milled orange glass

Name	Class		Date	Time	Duration					
Orange	Mining_LE_FP		14/12/2020	13:07:54	90.5 s					
Element	Al %	Si %	P %	S %	K %	Ca %	Ti %	V %	Mn %	Fe %
	1.88	34.00	0.22	1.04	0.17	11.38	0.44	0.24	0.05	0.36
±	0.071	0.105	0.016	0.020	0.006	0.017	0.005	0.043	0.009	0.009
Element	Cu %	Zn %	Rb %	Sr %	Zr %	Nb %	Mo %	Ba %	W %	
	0.01	0.02	0.00	0.05	0.06	0.00	0.01	0.40	0.09	
±	0.001	0.001	0.001	0.001	0.001	0.001	0.001	0.116	0.009	
Reference:										

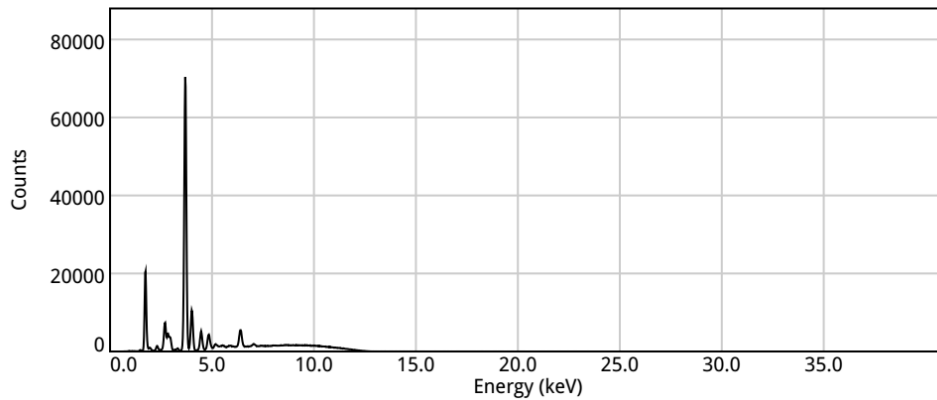
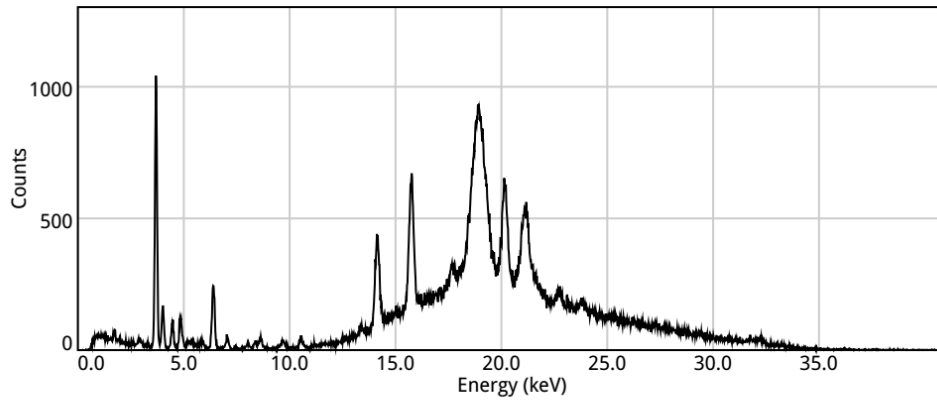


Fig. 6 XRF for milled orange glass

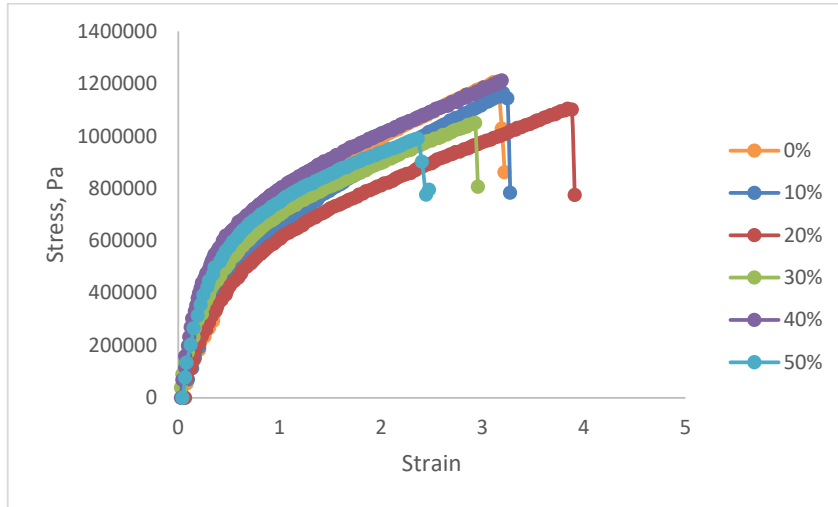


Fig. 7 Effect of filler concentration on the stress-strain of NBR composites

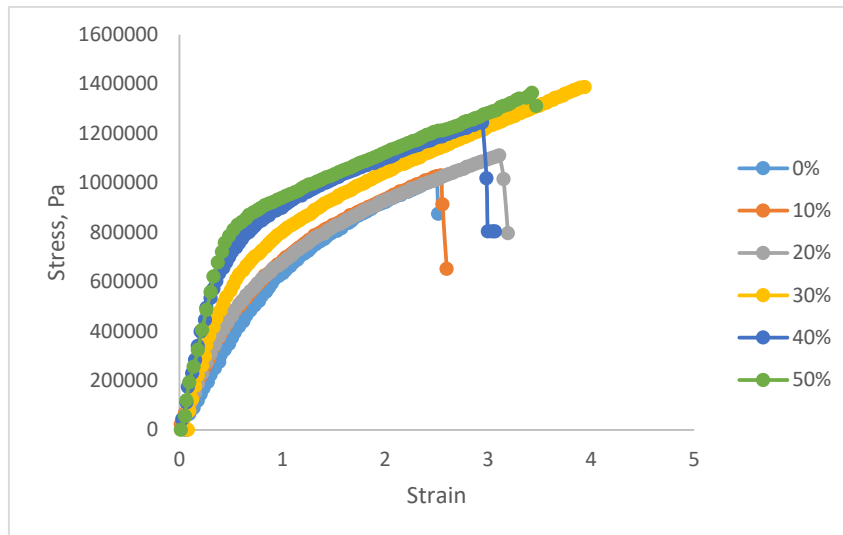


Fig. 8 Effect of filler concentration on the stress-strain of SBR composites

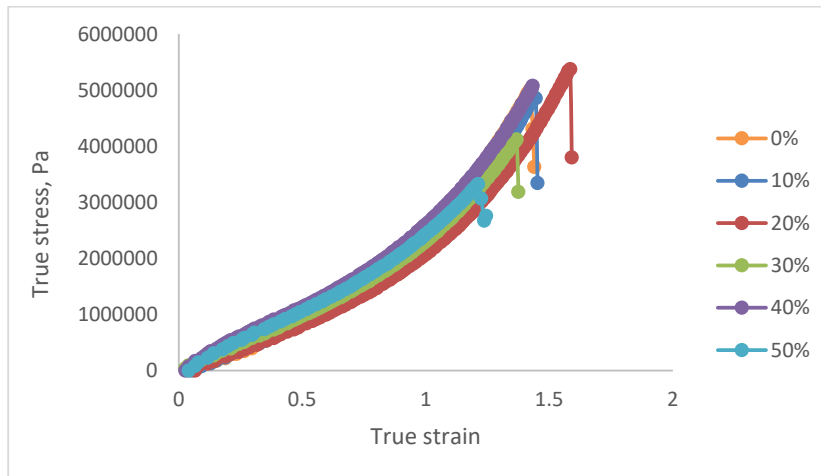


Fig. 9 True stress – True stain for micro glass-NBR composites

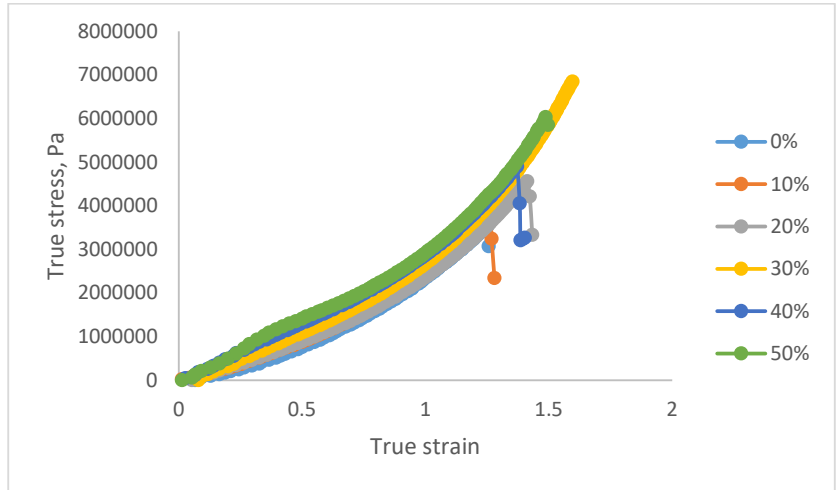


Fig. 10 True stress – True strain for micro glass-SBR composites

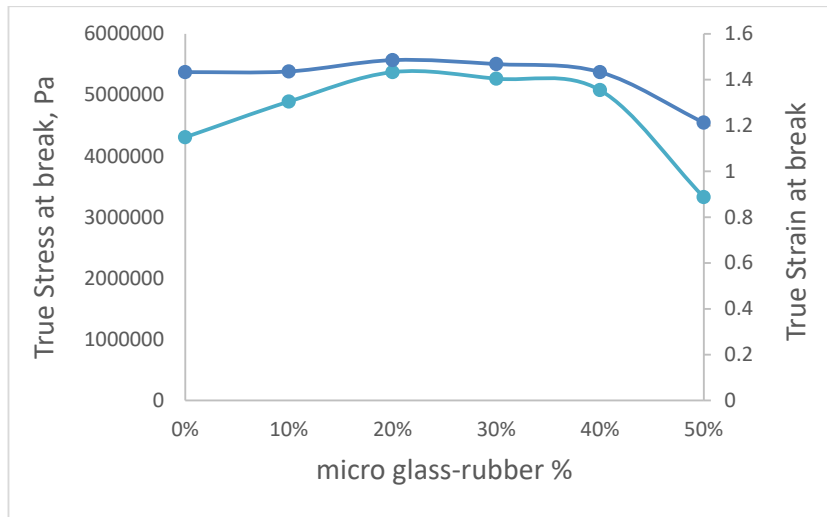


Fig. 11 True stress at break and true strain at break versus micro glass – NBR %

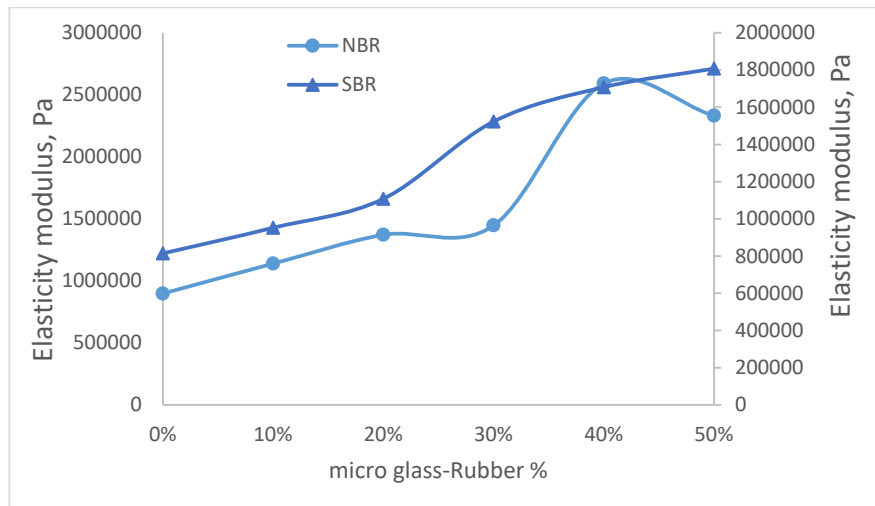


Fig. 12 Modulus of elasticity versus micro glass concentration for NBR and SBR composites

Table 1 NBR formulations with various micro orange glass concentrations

Ingradients	Phr ¹
NBR	100
ZnO	5
Stearic acid	2
Processing oil	10
MBTS ²	2
IPPD(4020) ³	1
Sulphur	2
Micro orange glass	0, 10, 20, 30, 40, 50

¹Part per hundred parts of rubber by weight

²MBTS: methylebenzthiazyle disulfide (accelerator)

³IPPD 4020: N-isopropyl-N'-phenyl-p-phenylene diamine (antioxidant, antiozonant, and antiflex)

Table 2 SBR formulations with various micro orange glass concentrations

Ingradients	Phr ¹
SBR	100
ZnO	5
Stearic acid	2
Processing oil	10
MBTS ²	2
IPPD(4020) ³	1
Sulphur	2
Micro orange glass	0, 10, 20, 30, 40, 50

¹Part per hundred parts of rubber by weight

²MBTS: methylebenzthiazyle disulfide (accelerator)

³IPPD 4020: N-isopropyl-N'-phenyl-p-phenylene diamine (antioxidant, antiozonant, and antiflex)

3. Results and discussion

3.1 Mechanical properties

The SEM, XRD, and XRF respectively shows the micrographs of the milled glass in range of 200 μm (b) SEM micrographs of the milled glass in range of 100 μm , and the chemical analysis with chemical phases as shown in Fig. 4, 5, and 6.

The Orange glass consists of Aluminum oxide (1.88%), Silicon oxide (34%), Phosphorus oxide (0.22%), Sulfur oxide (1.04%), potassium oxide (0.17%), calcium oxide (11.38%), Titanium oxide (0.44%), vanadium oxide (0.24%), manganese oxide (0.05%), Iron oxide (0.36%), copper oxide (0.01%), Zinc oxide (0.02%), Rubidium oxide (0.001%), Strontium oxide (0.05%), Zirconium oxide (0.06%), Niobium oxide (0.001%), molybdenum oxide (0.01%), Barium oxide (0.4%), Tungsten oxide (0.09%), shows an improvement in mechanical properties is attributed to a number of factors, including:

- 1- The strong interfacial interaction between the micro oxides particles and the rubber matrix.
- 2- The ability of the micro oxides particles to act as stress concentrators, which helps to reinforce the rubber matrix.
- 3- The small size of the micro oxides particles, which allows them to be more evenly dispersed in the rubber matrix.

These contributions of micro glass to enhance the mechanical properties of SBR and NBR rubber will discussed in the following paragraphs.

Figures 7, 8, and 9 shows the stress – Strain curve for selected concentrations of micro glass for NBR and SBR respectively. It is observed that as the concentration of micro glass increases the curves shifted toward higher values of stress with maximum shift at 40 phr for NBR and 50 phr for SBR. This result was also achieved from the values of true stress-true strain curves for NBR and SBR in fig. 10 and fig. 11 respectively.

True strain was obtained depending on the strain values using the following relation $\epsilon_t = \ln(1+\epsilon)$, while the true stress obtained depending on the values of stress and strain using the following relation $\sigma_t = \sigma(1+\epsilon)$. True stress-True strain figure ensures the relation between stress strain (fig. 10 and fig. 11).

Close examination of fig. 8 and fig.9 yields the following analyses:

- 1- The tensile strength of NBR composites is 40 phr for micro glass and 50 phr for SBR composites. This could be because the aggregation production of micro glass in the NBR matrix is more than in the SBR matrix.
- 2- It is observed that raising the micro glass content up to 40 phr boosts the reinforcing process by enhancing and increasing the crosslinking process between the elastomeric chains.
- 3- After reaching a level of 50 phr of micro glass, the tensile strength began to noticeably decline as more micro glass was added. This is because the presence of micro glass above 40 phr causes the production of micro glass aggregates of weak links between micro glass and NBR.
- 4- The slight reduction in elongation at break values that was seen when the micro glass content was increased may be explained by the restriction on polymeric chain movement brought on by the growth in micro glass aggregations. As a result, the

polymeric matrix may become stronger but more brittle. Fig. 12 illustrates this. As microglass concentrations rise above 40 phr in the NBR matrix, the strain at break is noticeably reduced.

Modulus of elasticity E for micro glass/NBR and micro glass/SBR composites presented in fig. 13. Fig. 13's behavior denotes a rise in elastic modulus with increasing micro glass content. The creation of glass aggregation, which is linked to agglomerates, increases as micro glass concentration rises. These aggregates may join together to form a secondary network that is continuous and kept together by Van der Waals or other attractive forces.

Additionally, it has been found that as the concentration of microglass in the NBR matrix is increased, the modulus of elasticity increases until it reaches a peak value at 40 phr, at which point it starts to decline. The network failure between the aggregates is blamed for this decrease. The strength of the network between the aggregates of micro glass inside the SBR matrix, however, may be the reason why a concentration of microglass in the matrix performs a high increment of the modulus of elasticity is observed at 40 phr.

Conclusions

In this research, the filler, Orange Glass powder was added to SBR/NBR blends in different proportions. Various physical properties of the compounds were experimentally investigated. The maximum values obtained for each of the mechanical properties Different results were obtained at different proportions of Orange Glass powder. Mainly, it is seen that most of the mechanical properties are showing maximum values at 40 phr. Therefore, in conclusion, SBR with 50% by weight of Orange Glass powder shows better combination of properties than other samples.

References

- [1]. A.A. Abdelsalam, S. Araby, S.H. El-Sabbagh, A. Abdelmoneim, M.A. Hassan, A comparative study on mechanical and rheological properties of ternary rubber blends, *Polym. Polym. Compos.* 29 (1) (2021) 15–28, <https://doi.org/10.1177/0967391119897177>.
- [2]. A. Remesh, G. Abhijith, P. Adwaith, S. Adithyan, S. Gopalan, N. Rahulan, Effect of boron carbide on physical properties of styrene butadiene rubber, *Mater. Today Proc.* 24 (2020) 2085–2093, <https://doi.org/10.1016/j.matpr.2020.03.665>.
- [3]. P. Naphon, S. Wiriyasart, N. Naphon, Thermal, mechanical, and electrical properties of rubber latex with TiO₂ nanoparticles, *Compos. Commun.* 22(2020) 100449, <https://doi.org/10.1016/j.coco.2020.100449>.
- [4]. M.A. Hassan, A. Aboul-Kasem, Mahmoud El-Sharief, Evaluation of the material constants of nitrile butadiene rubbers (NBR) with different carbon black (CB): FE-simulation and experimental, *J. Eng. Sci.* 38 (2010) 119–134, <https://doi.org/10.21608/jesaun.2010.123790>.
- [5]. M.D. Kiran, H.K. Govindaraju, T. Jayaraju, N. Kumar, Review-effect of fillers on mechanical properties of polymer matrix composites, *Mater. Today: Proc.* 5 (2018) 22421–22424, <https://doi.org/10.1016/j.matpr.2018.06.611>.
- [6]. V. Anandu, R. Sivaprasad, D. Dhudev, S. Kailas, N. Rahulan, Tensile and tear properties of boron carbide filled SBR/NBR blends, *AIP Conf. Proc.* 2281 (2020), <https://doi.org/10.1063/5.0028085020013>.
- [7]. Sadeghalvaad, Mehran, Dabiri, Erfan, Zahmatkesh, Sara, Afsharimoghadam, Pooneh. (2019). Improved curing conditions and mechanical/chemical properties of nitrile butadiene rubber

composites reinforced with carbon based nanofillers. *J. Nanostruct.* 9. 453–467. 10.22052/JNS.2019.03.007.

[8]. B. Alcock, J. Jørgensen, The mechanical properties of a model hydrogenated nitrile butadiene rubber (HNBR) following simulated sweet oil exposure at elevated temperature and pressure, *Polym. Test* 46 (2015) 50–58, <https://doi.org/10.1016/j.polymertesting.2015.06.010>.

[9]. K. Akshay, M. Arjun, S. Govind, V. Hrithwik, S. Akhil, N. Rahulan, Mechanical behavior of silicon carbide filled SBR/NBR blends, *Mater. Today: Proc* 42 (2021), <https://doi.org/10.1016/j.matpr.2021.01.234>.

[10]. S. Yadav, N. Guntur, N. Rahulan, S. Gopalan, Effect of titanium carbide powder as a filler on mechanical properties of silicone rubber, *Mater. Today: Proc.*(2021), <https://doi.org/10.1016/j.matpr.2020.11.714>.

[11]. R. Harikrishnan, T.P. Mohan, N. Rahulan, S. Gopalan, Effect of silicon nitride on physical properties of SBR, *Mater Today: Proc* 43 (2020), <https://doi.org/10.1016/j.matpr.2020.11.421>.

[12]. A. Thabet, A. Abouel-Kasem, M. Bayoumi, M. El-Sebaie, Insight into the effect of CB loading on tension, compression, hardness and abrasion properties of SBR and NBR filled compounds, *Mater. Des.* 30 (2009) 1785–1791, <https://doi.org/10.1016/j.matdes.2008.07.037>.

[13]. M. Nasir, B.T. Poh, P.S. Ng, Effect of c-mercaptopropyltrimethoxysilane coupling agent on T90, tensile strength and tear strength of silica-filled NR, NBR and SBR vulcanizates, *J. Eur. Polymer* 24 (10) (1988) 961–965, [https://doi.org/10.1016/0014-3057\(88\)90177-2](https://doi.org/10.1016/0014-3057(88)90177-2).

[14]. Amir Elzawwy, Y.H.Elbashar, “Study of free radical polymerization of chitosan reinforced N- isopropylacrylamide/Acrylamide (NIPAM/AAM) composites directed towards bio-applications”, *nonlinear optics and quantum optics, NLOQO Volume 57, Number 1-2 (2023)*, p. 81-97

[15]. Mai S. Ismail, A. A. Elamin, F. Abdel-Wahab, Y.H.Elbashar, M. M. Mahasen, “Improving the Refractive Index by Engineering PbS/PVA Nano Polymer Composite for Optoelectronic Applications”, *Optical Materials* 131 (2022) 112639, 1-8

[16]. D.I. Moubarak, H. H. Hassan, T.Y. El-Rasasi, H. S. Ayoub, A.S. Abdel-Rahaman, S. A. Khairy, Y. H.Elbashar, "Internal Friction of Nano-Sized Carbon Black-Loaded Polymeric Composites Using Laser Shadowgraphic technique: A Review", *Journal of Nonlinear Optics and Quantum optics, NLOQO Volume 53, Number 1-2 (2020)*, p. 31-59

[17]. D. I. Moubarak, M. A. Abd Al-Halim, A. Abu-Hashem, Y. Elbashar, "Study of Surface Treatment of Polyester by Plasma processing", *Journal of Nonlinear Optics and Quantum optics, NLOQO Volume 52, Number 3-4 (2020)*, p. 325-336

[18]. D. I. Moubarak, M. A. Abd Al-Halim, A. Abu-Hashem, Y. Elbashar, “Study of DC Pseudo Plasma Processing for Surface Treatment of Polyester”, *Physics AUC*, vol. 29, 50-60 (2019)

[19]. D. I. Moubarak, M. A. Abd Al-Halim, A. Abu-Hashem, and Y.H. Elbashar, "AFM and SEM analysis of polystyrene Surface Treated by DC Pseudo Plasma Discharge", *Egyptian Journal of Chemistry*, 2019, DOI: 10.21608/EJCHEM.2019.5365.1473, Article 13, Volume 62, Issue 7, July 2019, pp1335-1341

[20]. D.I. Moubarak, J. A. Khaliel, T.Y. El-Rasasi, H. S. Ayoub, A.S. Abdel-Rahaman, S. A. Khairy, H. H. Hassan, Y.H. Elbashar, “Mechanical and laser shadowgraphy studies of nanosized carbon black loaded natural rubber”, *Lasers in Engineering*, 2018III08.Modi-JL, 2019, LIE 43.4-6, p. 201-212

[21]. Hussam Hassan, Deia Moubarak, Jamal Khaliel, Hany Ayoub, Ahmed Abdel-Rahaman, Sherif Khairy, Tarek El-Rasasi, Yahia Elbashar, “Design and construction of optical laser shadowgraphy system for measuring the internal friction of high elasticity solids”, *Journal of Nonlinear Optics and Quantum optics (NLOQO)*, Volume 48, Number 4 (2018), p. 313-320